Neuroscience 300 (2015) 554–565

THETA FREQUENCY PREFRONTAL–HIPPOCAMPAL DRIVING RELATIONSHIP DURING FREE EXPLORATION IN MICE

Y. ZHAN *

Brain Cognition and Brain Disease Institute, Shenzhen Institutes of Advanced Technology, Chinese Academy of Sciences, Shenzhen 518055, China

Mouse Biology Unit, European Molecular Biology Laboratory, Monterotondo 00015, Italy

Abstract—Inter-connected brain areas coordinate to process information and synchronized neural activities engage in learning and memory processes. Recent electrophysiological studies in rodents have implicated hippocampal–prefrontal connectivity in anxiety, spatial learning and memory-related tasks. In human patients with schizophrenia and autism, robust reduced connectivity between the hippocampus (HPC) and prefrontal cortex (PFC) has been reported. However little is known about the directionality of these oscillations and their roles during active behaviors remain unclear. Here the directional information processing in mice was measured by Granger causality, a mathematical tool that has been used in neuroscience to quantify the oscillatory driving relationship between the ventral HPC (vHPC) and the PFC in two anxiety tests and between the dorsal HPC (dHPC) and the PFC in social interaction test. In the open field test, stronger vHPC driving to the PFC was found in the center compartment than in the wall area. In the light–dark box test, PFC to vHPC causality was higher than vHPC to PFC causality although no difference was found between the light and dark areas for the causality in both directions. In the social interaction test using *Cx3cr1* knockout mice which model for deficient microglia-dependent synaptic pruning, higher PFC driving to the dHPC was found than driving from the dHPC to the PFC in both knockout mice and wild-type mice. *Cx3cr1* knockout mice showed reduced baseline PFC driving to the dHPC compared to their wild-type littermates. PFC to dHPC causality could predict the actual time spent interacting with the social stimuli. The current findings indicate that directed oscillatory activities between the PFC and the HPC have task-dependent roles during exploration in the anxiety test and in the social interaction test.

Key words: Granger causality, theta oscillation, social interaction, anxiety, local field potential.

INTRODUCTION

The synchronization between the prefrontal cortex (PFC) and hippocampus (HPC) is thought to facilitate communications between two structures. Theta rhythms have been shown to be selectively enhanced between the PFC and HPC during mnemonic processes (Jones and Wilson, 2005; Benchenane et al., 2010). In these memory tasks when the animals acquired the task rules neurons in the PFC and HPC were more correlated and PFC neuron firing was locked to HPC theta phase of local field potentials (LFPs). Such modulations of PFC neuron activities may reflect the inputs of spatial-related information from the HPC, a structure critical for encoding location and navigation (Buzsáki, 2002; Bird and Burgess, 2008), into the PFC which regulates attention and decision making (Miller and Cohen, 2001; Dalley et al., 2004). In anxiety-related behaviors, vHPC activities were correlated with the PFC and the correlation was enhanced in the anxiogenic environments (Adhikari et al., 2010). In the anxiety test using elevated-plus maze, PFC neurons were modulated by ventral HPC theta oscillations and these PFC neurons were inversely correlated with anxiety-related measures (Adhikari et al., 2011).

The underconnectivity theory has proposed that autism is a cognitive disorder marked by underfunctioning integrative circuitry that results in deficient integration of information at the neural and cognitive levels (Courchesne et al., 2005; Just et al., 2012). Similarly, the disconnection hypothesis in schizophrenia also attributes the pathophysiology of the disease to the disrupted synaptic efficacy at circuitry level (Friston, 1999; Pettersson-Yeo et al., 2011). Using a genetic mouse model of schizophrenia which captured chromosomal deficiency to model human chromosome 22 (22q11.2) microdeletion, it was shown that *Df*(*16*)$A^{+/-}$ mice had reduced synchronization between the dHPC and the PFC (Sigurdsson et al., 2010). Theta frequency LFP coherence between the two areas also predicted the learning performance in these mice. In another mouse model of deficient synaptic pruning by microglia, *Cx3cr1* knockout mice showed reduced dHPC–PFC coherence and the coherence was correlated with social behavior (Zhan et al., 2014). Considering the commonly reported connectivity deficits in human brain-

*Address: The Brain Cognition and Brain Disease Institute, Shenzhen Institutes of Advanced Technology, Shenzhen 518055, China. Fax: +86-(0)755-86392299.
E-mail address: yang.zhan@siat.ac.cn

Abbreviations: ANOVA, analysis of variance; AR, autoregression; HPC, hippocampus; LFPs, local field potentials; PBS, phosphate-buffered saline; PFC, prefrontal cortex.

http://dx.doi.org/10.1016/j.neuroscience.2015.05.063
0306-4522/

imaging studies in schizophrenia (Uhlhaas and Singer, 2010) and autism (Schipul et al., 2011), reduction in synchronized rhythmic activities may contribute to the cognitive dysfunctions and impaired information processing that requires coordination of long-range brain structures.

In this study LFP signals were recorded from the HPC and PFC in free moving mice using a wireless data logging system. Granger causality was used to address the driving relationship between the HPC and the PFC. The Granger causality was modeled as bivariate time series and estimated using autoregression (AR) model. In the open-field test and the light–dark box test, the Granger causality was analyzed between the vHPC and the PFC. In the social interaction test the causality was analyzed between the dHPC and the PFC. It was shown that directed causal influence from the vHPC to the PFC was associated with anxiety-related behavior and PFC causal influence to the dHPC could predict social behavior.

EXPERIMENTAL PROCEDURES

Animals

Two separate cohorts of male mice were used in the anxiety tests and the social interaction test respectively. For the open-field test and the light–dark box test, C57BL/6J mice were purchased from Charles River Laboratories (Calco, Italy) and housed in ventilated cages. For the social interaction test, *Cx3cr1* knockout mice were obtained from internal EMBL breeding colony. The *Cx3cr1* knockout mice also carried a *Thy1*::*GFP* transgene and they were on a C57BL/6J congenic background (Zhan et al., 2014). Animals were kept on a 12-h light, 12-h dark cycle (lights on at 7 a.m.) with ambient temperature (21.5 ± 1 °C) and humidity (55 ± 8%). Food and water were available *ad libitum*. This study was approved by the animal ethics committee of EMBL and the Italian Ministry of Health and experiments were carried out in accordance with the National Institutes of Health guide for the care and use of laboratory animals.

Surgery

Three-to-six-month-old mice were used for the electrophysiological recording experiments. Mice were anesthetized with a mixture of ketamine and xylazine (100 mg/kg and 10 mg/kg) and placed on a heating pad which maintains the body temperature at 35 °C. The head was fixed on a stereotaxic frame with microscope. Supplemental inhaling isofluorine was provided. An incision above the mouse skull was cut and burr holes were drilled at the locations of dHPC (using bregma as reference and the depth is relative to the brain surface, 1.9 mm posterior, 1.4 mm lateral and 1.35 mm depth), vHPC (3.1 mm posterior, 3.2 mm lateral, and 3.9 mm depth) and PFC (1.8 mm anterior, 0.5 mm lateral and 1.5 mm depth). Tungsten wire electrodes (Advent Research Materials, Oxford, UK) were advanced into the brain at the above locations and these coordinates aimed at the dorsal CA1 region of HPC, the ventral part of HPC and the deep layer of medial PFC. Two additional micro screws were anchored on the posterior and anterior portions of the skull as ground and reference, respectively. The electrode wires were inserted into a 7-pin connector which serves as an interface for Neurologger recording and dental cement was carefully applied over the skull to form a headstage that protected the electrodes and wiring. After surgery, animals were housed individually and allowed at least 1 week to recover.

Open-field test

Before the test, the animals were habituated to the handling of putting on the Neurologger for three consecutive days. A dummy Neurologger with the similar shape and weight was fitted to the headstage and remained on the animal's head for at least 10 min each day. The open-field was a round arena with diameter 40 cm and the wall 20 cm. The 5-min test was started by placing the mice in the center and behavior was recorded and tracked by Viewer2 video-tracking systems (Biobserve, St. Augustin, Germany).

Light–dark box test

The light–dark box consisted of a 40 cm by 40 cm Plexiglas box in which half of the chamber contained the dark compartment. The same group of mice from the open-field test were used and the light–dark test was performed 1 week after the open-field test. The dummy Neurologger was habituated to the animal before the test. The 10-min test was started by placing the mice in the center of the light area and the mice were tracked by Viewer2 video-tracking systems.

Social interaction test

Similar habituation handling was also done before the social interaction test. The test apparatus consisted of a three-compartment box with separating plates that had opening doors for the animals to go through the compartments. Metal wire mesh tubes were placed into the outside compartments away from the door, and a same-sex juvenile (P21–P24) mouse was placed into one of the two tubes. The test started with a 5-min free exploration of the test apparatus and followed by a 10-min social interaction period. The behavior of the mice was video-tracked by Viewer2 software.

Data acquisition

Electrophysiological recordings were acquired via the wireless Neurologger system (Vyssotski et al., 2009). The LFP data were recorded wirelessly and logged onto the memory card simultaneously on the Neurologger and this ensured stable and good quality recordings. After the experiments the data were downloaded to a computer offline. The Neurologger 2A device (Brankačk et al., 2010; Zhan et al., 2014) was small and light with the weight about 2 g and the additional animal headstage was only about 1 g. The Neurologger had four recording channels and only LFP recording options were available

at the time of recordings. The LFP data were sampled at 1600 Hz and after the experiments the data were imported into the computers for analysis. The Neurologger had an infrared receiver on board and a synchronizing event was sent to the Neurologger and the video-tracking computer to mark both the behavioral tracking data and the recorded LFPs (Etholm et al., 2010). The examples of LFP traces are shown in Fig. 1A. In this report, LFP data published in (Zhan et al., 2014) were re-used for Granger causality analysis.

Data analysis

Data were analyzed using Matlab. The behavioral tracking data (25 fps) in the open field test, the light–dark box test and social interaction test were first analyzed using SEE Workshop (Lipkind et al., 2004). The SEE software used a LOWESS algorithm to smooth the tracking position data (Hen et al., 2004). For the open-field test, the SEE software also partitioned the tracking data of each mouse into wall and center based on an algorithm estimating circular wall and radial distance (Lipkind et al., 2004). In the open-field test, the speed range of animal was separated into 0–5 cm/s, 5–10 cm/s and 10–15 cm/s. For the majority of time the animals' speed fell into the range of 5–10 cm/s and LFP data in the speed range of 5–10 cm/s were used. In the social interaction test, the speed range 0–5 cm/s was used and the LFP power was not affected significantly by the speed (Zhan et al., 2014).

Directionality of the oscillatory information between HPC and PFC was analyzed by Granger causality in the frequency domain (Brovelli et al., 2004; Ding et al., 2006). The prefrontal and hippocampal LFP data and their dependency were modeled as bivariate autoregressive (AR) processes. The estimates of the AR coefficient matrix were done by solving the Yule–Walker equation using Levinson, Wiggins and Robinson algorithm (Proakis and Manolakis, 1996; Ding et al., 2000). The choice of the model order was accessed by Akaike Information Criterion (AIC) (Akaike, 1974). After the model was fit, the AR coefficients and the covariance were used to estimate the power spectrum and coherence. Before AR model fitting and spectral analysis, the data were downsampled to 200 Hz and filtered at 1–90 Hz using a third order Chebyshev 1 filter. The estimated LFP power and coherence were also compared with the Fourier-based periodogram methods. In the open-field test and the light–dark box test the model order was chosen as 9 and 30, respectively. In the social interaction test the order was chosen as 20. The periodogram method used a Hanning window of 200 data points with 50% overlap. Granger causality value was calculated as the mean of the chosen frequency range. The power was calculated as the sum of the chosen frequency range.

Histology

At the end of the experiments, mice were deeply anesthetized and electrolytic lesions were made by a lesion making device (Ugo Basile, Comerio, Italy). Mice were then perfused transcardially with phosphate-buffered saline (PBS) and 4% phosphate-buffered paraformaldehyde. Brains were dissected out, post fixed overnight at 4 °C and cryoprotected (30% sucrose in PBS, 4 °C). The brains were frozen and sections were obtained on a cryostat (Leica Microsystems, Wetzlar, Germany) at 40 µm. Sections including the dorsal HPC were mounted on glass slides and stained using the Nissl technique with 0.1% Cresyl Violet to determine the location of recording electrodes. Examples of the electrode tips are shown in Fig. 1B.

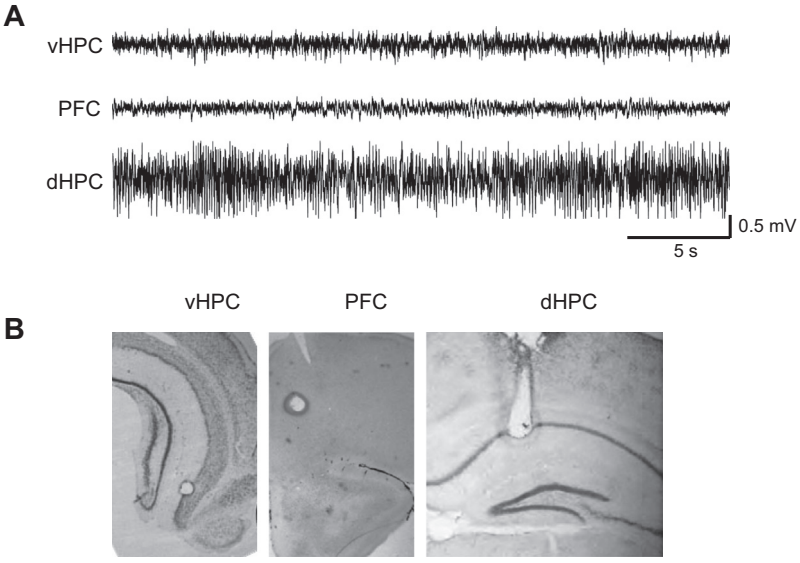

Fig. 1. (A) Representative 30-s LFP recordings from wireless Neurologger in three brain areas of vHPC, PFC and dHPC in free moving mice during open field and social interaction test. (B) Schematic representations of coronal sections showing positions of the recording electrode tips in vHPC, PFC and dHPC.

RESULTS

To make sure that the AR model was a good fit to estimate the Granger causality, power estimations using the parametric AR models (Fig. 2A) and the Fourier-based periodogram methods (Fig. 2B) were compared. The two methods yielded very similar results for vHPC power, PFC power and the coherence (Fig. 2) between the vHPC and PFC in the open-field test. The Granger causality depends on the successful identification of a proper model to make predictions, hence comparing the spectral estimate using AR methods to that of the Fourier-based methods guaranteed a proper selection of the order for causality estimates.

vHPC → PFC causality in the center is higher than near the wall in the open field

The open-field test is frequently used for screening motor functions and anxiety in rodents. The peripheral and the center areas are two major components for behavioral analysis. Behavioral tracking data were separated into center and peripheral wall areas (Fig. 3A). More time spent in the center indicated a less anxious state. Over the 5-min test, the mice spent 27.1% ± 3.7% (mean ± s.e.m.) of time in the center. The causality of LFPs between the vHPC and the PFC in the wall areas and in the center areas were calculated respectively (Fig. 3B, C). At theta frequency range, causality from the vHPC to the PFC was higher during the exploration of center area than the exploration near the wall (Fig. 3D, t_{26} = 2.6, P = 0.01), however causality from the PFC to the vHPC in the center area was not different from that in the wall area (Fig. 3D, t_{26} = 1.01, P = 0.3). The higher vHPC → PFC causality was not related with the changes in power as theta power in the wall area was not from the power in the center area in both vHPC (Fig. 3E, t_{26} = 0.07, P = 0.95) and PFC (Fig. 3F, t_{26} = 0.09, P = 0.93). Previous study measuring the correlation between vHPC and PFC theta power has found an increased power correlation in the center area (Adhikari et al., 2010). Theta oscillations might coordinate the anxiety behavior through the synchronization between the vHPC and the PFC, and using causality analysis stronger theta vHPC → PFC driving was found demonstrating that directional information was flowing out of the vHPC recruiting the vHPC–PFC pathway in the open-field test.

PFC → vHPC causality is higher than vHPC → PFC causality in light–dark box test

To further examine the driving relationship between the vHPC and the PFC during anxiety, theta causality was measured in another anxiety test of light–dark box test. The mice spent 21.4 ± 3.2% of time in the light area of the 10-min test indicating that the mice preferred to stay in the dark area of the test box, similar to the previous reports using this test (Bourin and Hascoët, 2003). Similarly, the power and coherence estimates using the AR method (Fig. 4A) and periodogram method (Fig. 4B) were compared. These two methods produced very similar results. Then the causality between the vHPC and the PFC was calculated during the light–dark box test (Fig. 5A). The average Granger causality estimations for vHPC → PFC and PFC → vHPC directions are shown in Fig. 5B, C respectively. During the exploration of both the dark and light phases of the test, the PFC → vHPC theta causality was higher than the vHPC → PFC causality (Fig. 5D; repeated measures analysis of variance (ANOVA), $F_{(1,16)}$ = 22.31, P = 0.0002). This indicates that theta oscillations in the PFC drove the vHPC theta

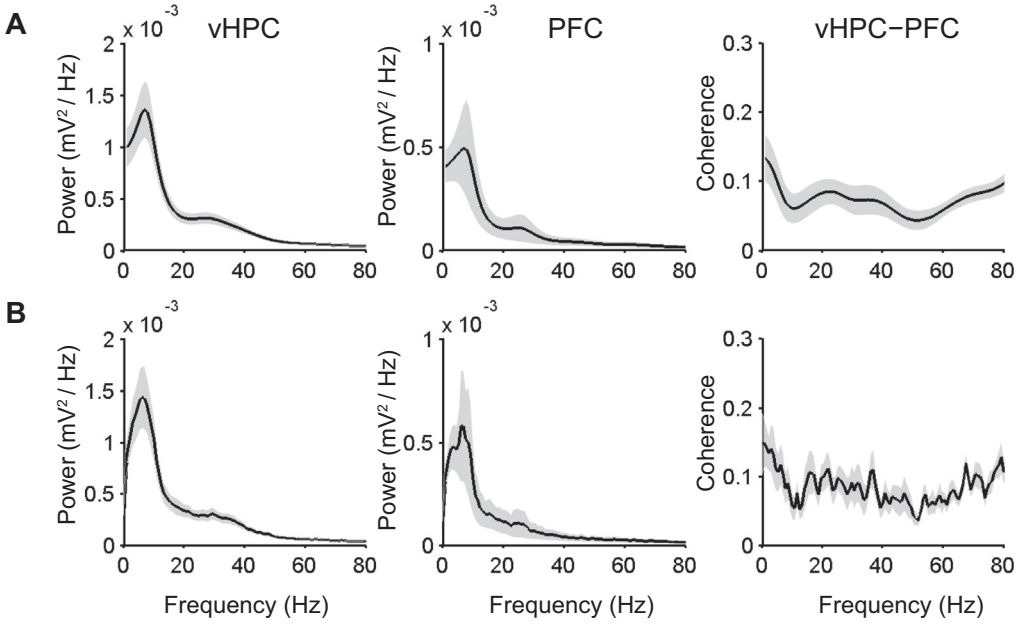

Fig. 2. Power spectra and coherence using (A), AR methods and (B), periodogram methods when the mice were exploring the open field. Left column, power spectrum in vHPC; middle column, power spectrum in PFC; right column; coherence between vHPC and PFC. Power spectra and coherence were averaged across animals (N = 14) and the curves and the shaded areas indicate mean ± s.e.m.

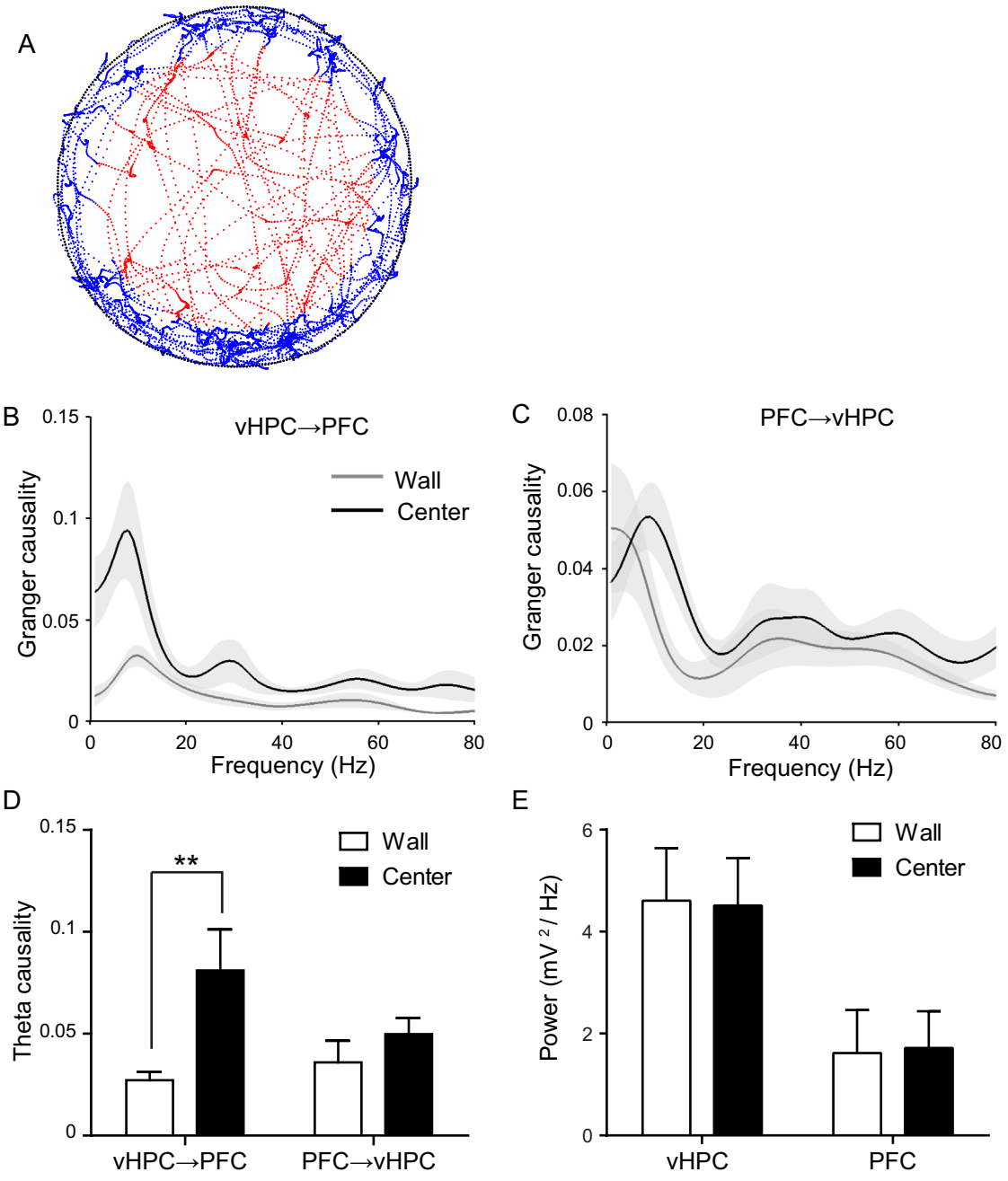

Fig. 3. Causality between vHPC and PFC during open field test (N = 14). (A) Representative video tracking data in an open field. The center (red) area, the peripheral area (blue) and the wall (black) were estimated using SEE software. (B) and (C) Average Granger causality for both vHPC → PFC and PFC → vHPC directions. (D) Theta band (4–12 Hz) causality in the wall and center areas. The vHPC → PFC causality was higher in the center area than in the wall area. (E) Theta power for the vHPC and the PFC in the center and wall areas. Neither vHPC nor PFC power showed difference in the two areas. $^{**}P < 0.01$. (For interpretation of the references to color in this figure legend, the reader is referred to the web version of this article.)

activities when the mice navigated the environment. However, no difference was found for the vHPC → PFC theta causality between the light phase and the dark phase (Fig. 5B, D; $t_{16} = 1.04$, $P = 0.31$). Additionally, there was also no difference for the PFC → vHPC causality between the two phases (Fig. 5C, D; $t_{16} = 0.69$, $P = 0.5$). The higher PFC driving to the vHPC was not related with the magnitude of the power, as theta power showed no difference between the dark phase and the light phase in both vHPC (Fig. 5E; $t_{16} = 0.39$, $P = 0.7$) and PFC (Fig. 5E; $t_{16} = 0.28$, $P = 0.78$) areas.

PFC → dHPC causality is higher than dHPC → PFC causality in social interaction test

In the social interaction test, mice were tested in a three-chambered box (Fig. 7A) in which the mice spent 5 min habituating the box and then 10 min interacting with a

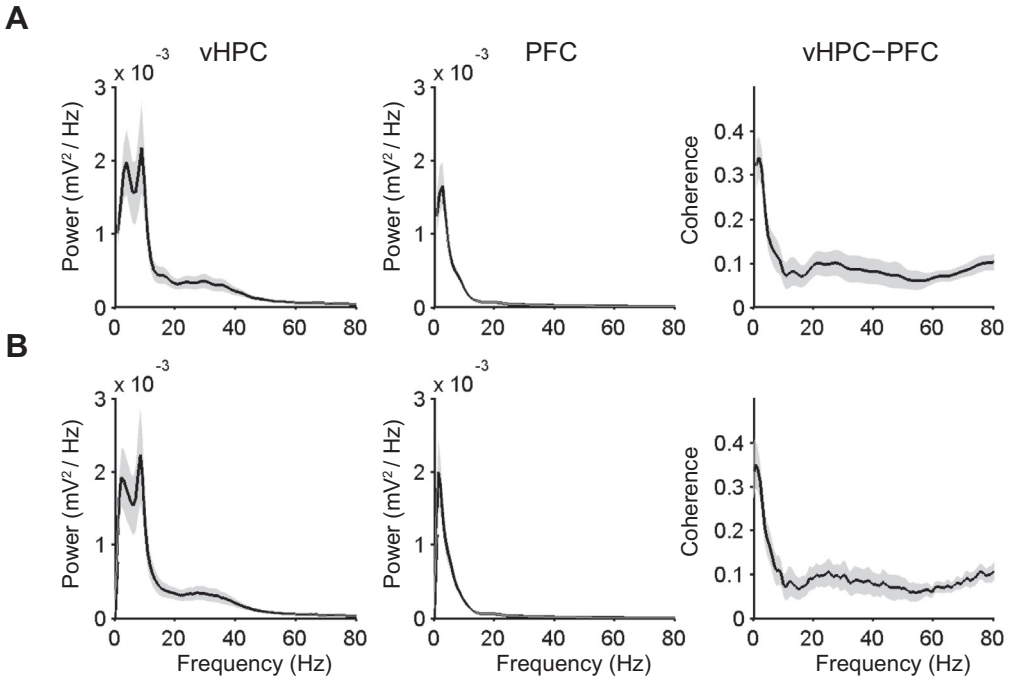

Fig. 4. Power spectra and coherence estimation using (A), AR method and (B), periodogram method during the exploration in the light–dark test. Left column, power spectrum in vHPC; middle column, power spectrum in PFC; right column; coherence between vHPC and PFC. Power spectra and coherence were averaged across animals ($N = 9$) and the curves and the shaded areas indicate mean ± s.e.m.

social stimulus. Before the application of Granger causality spectral estimation using the AR method (Fig. 6A) and the periodogram method (Fig. 6B) were analyzed. Comparing the two methods, power spectra and coherence were very similar in both wild-type and *Cx3cr1* knockout mice (Fig. 6) and this gave the same results of reduced coherence as found in *Cx3cr1* knockout mice previously (Zhan et al., 2014). Then causality relationships were measured between the PFC and the dHPC during both habituation (Fig. 7B, C) and social interaction phase (Fig. 7D, E). There was a pronounced theta activity at both directions between the dHPC and the PFC. Theta causality for PFC → dHPC was higher than dHPC → PFC causality during both habituation (Fig. 7F, repeated measures ANOVA, $F_{(1,15)} = 29.43$, $P < 0.0001$) and social interaction (Fig. 7G, $F_{(1,15)} = 19.62$, $P = 0.0005$) phase in both knockout and wild-type animals, indicating a consistent causal influence from the PFC to the dHPC throughout the test.

Reduced PFC → dHPC driving in *Cx3cr1* knockout mice

Stronger PFC → dHPC theta causality in both *Cx3cr1* knockout mice and their wild-type littermates revealed that oscillatory driving is mainly coming from the PFC, an area implicated in attentional functions such as attention to stimulus features (Dalley et al., 2004). Synchronization measurements between genotypes showed reduction of PFC–dHPC coherence across a range of frequencies (Zhan et al., 2014). Then PFC → dHPC causal relationships in *Cx3cr1* knockout and wild-type mice were compared. Wild-type, but not *Cx3cr1* knockout mice showed higher theta PFC → dHPC causality during the baseline habituation period (Fig. 7C, F, causality × genotype, $F_{(1,15)} = 4.95$, $P = 0.04$, Bonferroni correction), indicating a reduced PFC → dHPC causality in *Cx3cr1* knockout mice. During the social interaction phase, *Cx3cr1* knockout mice showed a non-significant smaller PFC → dHPC causality than the wild-type mice (Bonferroni correction, Fig. 7E, G). The failure of an intact baseline PFC to dHPC information flow might reflect the inability of *Cx3cr1* knockout mice attending to a social stimulus. To investigate the functional role of PFC to dHPC causal influences, the correlation between the time spent interacting with the social stimuli and theta band PFC → dHPC causality was calculated. Indeed there was a significant correlation between the social interaction time and the baseline PFC → dHPC causality (Fig. 8A, $r = 0.65$, $P = 0.005$) during habituation indicating that baseline causal influences from the PFC to the dHPC could predict the social behavior in the future. Such behavioral correlation was not found in the dHPC → PFC causality (Fig. 8B, $r = -0.22$, $P = 0.39$). Additionally the causality during the social interaction phase was not correlated with the duration of social interaction (Fig. 8C, D). These data revealed a role of PFC → dHPC causal influence during social interaction.

DISCUSSION

Using a wireless recording technique in free-behaving mice and the analysis of Granger causality analysis, higher causal influences from the vHPC to the PFC

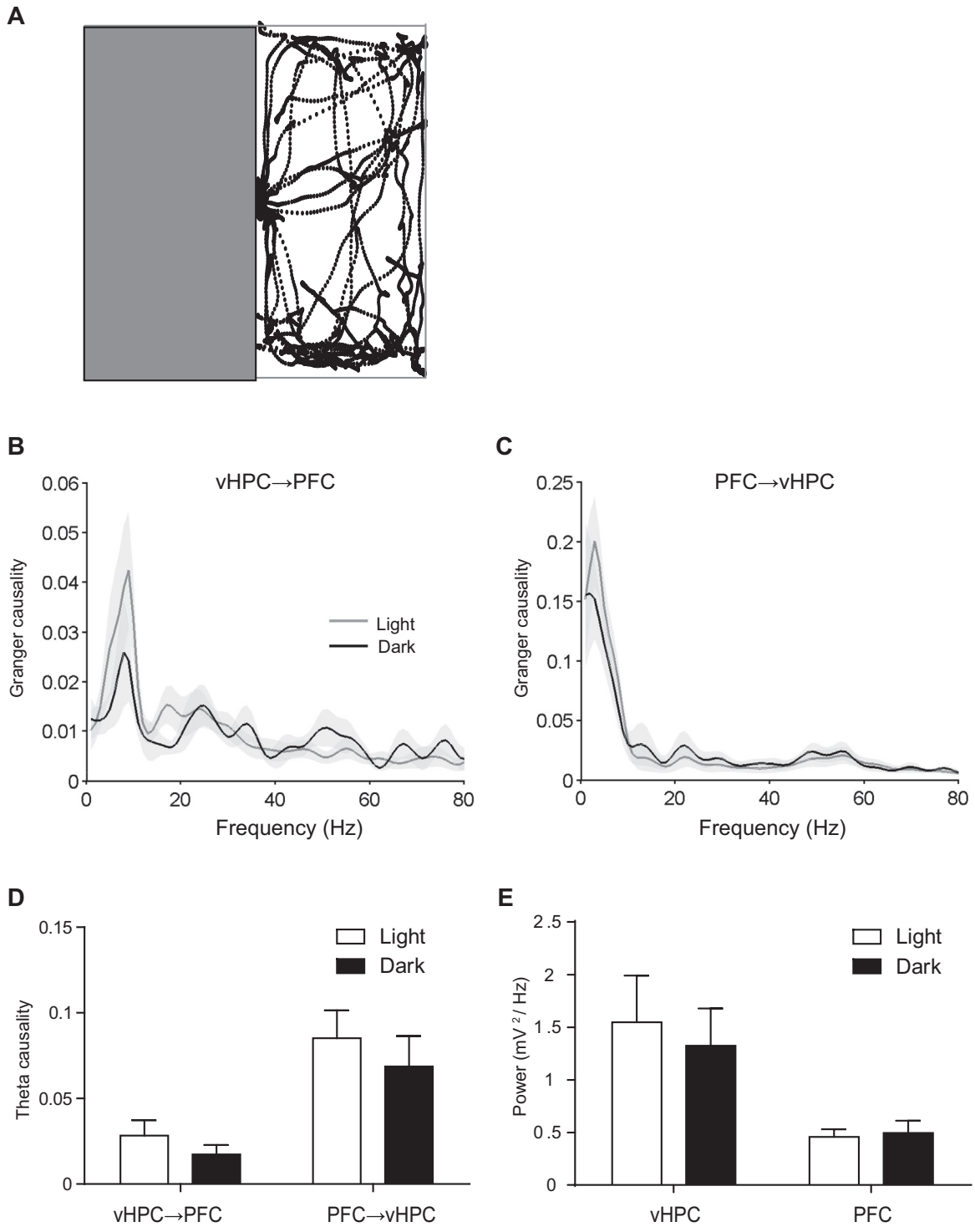

Fig. 5. Causality between the vHPC and PFC in the light–dark box ($N = 9$). (A) Light–dark box test and the representative tracking behavioral trace. (B) and (C) Theta band (4–12 Hz) causality in the dark and light areas in both vHPC → PFC (B) and PFC → vHPC (C) directions. The causality in the light area was not different from that in the dark area in either PFC → vHPC or vHPC → PFC direction. (D) Average theta band PFC → vHPC and vHPC → PFC causality during light and dark phase. PFC → vHPC causality was higher than vHPC → PFC causality. (E) Average theta power for vHPC and PFC in the light and dark areas. In the two areas, no difference was found for vHPC and PFC power.

were found in the center area than in the wall area in the open-field test. While major direction of causal driving was from the PFC to the vHPC rather than from the vHPC to the PFC in the light–dark test, there was no difference between the light phase and the dark phase for the causal influences in both directions. In the social interaction test, it was found that PFC driving to the dHPC was more prominent than driving from the dHPC

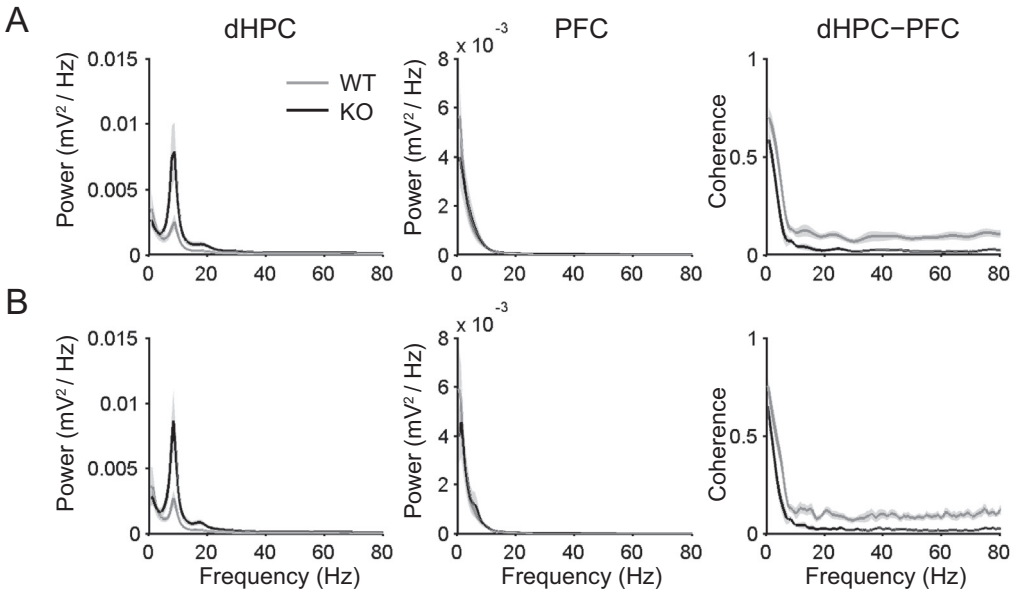

Fig. 6. Power spectra and coherence using (A), AR method and (B), periodogram method when the *Cx3cr1* knockout mice and wild-type mice were exploring the three-chambered box during the habituation phase of social interaction. Left column, power spectrum in dHPC; middle column, power spectrum in PFC; right column; coherence between dHPC and PFC. Power spectra and coherence were averaged across animals (KO (knockout): $N = 10$; WT (wild-type): $N = 7$) and the curves and the shaded areas indicate mean ± s.e.m.

to the PFC. *Cx3cr1* mice, a mouse model with reduced synaptic pruning mediated by microglia, showed reduced PFC to dHPC causal influences during habituation period in the social interaction test. The baseline PFC → dHPC causality could predict the social behavior.

Ventral HPC in anxiety

The vHPC is thought to play an important role in regulating anxiety (McHugh et al., 2004; Engin and Treit, 2007). Lesions in the vHPC decreased anxiety-related behavior in anxiety tests (Kjelstrup et al., 2002). Recordings of LFPs in both PFC and vHPC showed increased correlation between the theta power in the two structures in elevated-plus maze and open field, suggesting a stronger coordinated power fluctuation in the two areas (Adhikari et al., 2010). In this study the Granger causality was used to specifically test that whether LFP measurement in the past observation in either HPC or PFC can predict the observation in another area. Statistically the ''Granger causal'' refers to the reduction of the prediction error by use of a linear multivariate model (Seth, 2010).

In the open-field test, stronger vHPC causal influences to the PFC were found in the anxiogenic environments, suggesting that the information flowing out of the vHPC modulates anxiety. Anatomically the vHPC projects directly to medial PFC (Hoover and Vertes, 2007). Stronger vHPC driving to the PFC in the open-field test clearly could take advantage of this direct synaptic pathway. A recent study using optogenetics showed that optically activating granule cells in the ventral part of dentate gyrus in the HPC produced less anxious state in mice with more traveling in the center of the open field (Kheirbek Mazen et al., 2013). Stronger driving from the vHPC may reflect that processing of contextual anxiety-related information passes down to the downstream targets, possibly involving other anxiety-related regions such as amygdala (Kishi et al., 2006; Bienvenu Thomas et al., 2012) or lateral septum (Trent and Menard, 2010; Anthony Todd et al., 2014).

In the light–dark box test, theta causality for both vHPC → PFC and PFC → vHPC directions showed no difference between the dark and the light phases. This result shows that directional driving between the PFC and the vHPC is not sensitive to the anxiogenic compartments in the test assay. However, the PFC to vHPC causality was higher than the vHPC to PFC causality throughout the test, indicating that the major directional driving was from the PFC to the vHPC when the mice explored the dark and light areas. The PFC also has been implicated in anxiety and previous reports found that inactivation of the PFC by muscimol or excitotoxic acid produced anxiolytic effects in the elevated plus maze (Shah and Treit, 2003; Shah et al., 2004).

PFC in social interaction

In the social interaction test, PFC driving to the dHPC was more prominent than dHPC driving to the PFC in both *Cx3cr1* knockout and wild-type mice, suggesting that processing of information flows out of the PFC. Top–down processing requires the PFC when behavior needs to be guided by internal states or intentions (Miller and Cohen, 2001; Amodio and Frith, 2006). Previously in *Cx3cr1* knockout mice decreased theta band PFC–dHPC coherence was found (Zhan et al., 2014) and in this report it was further found that

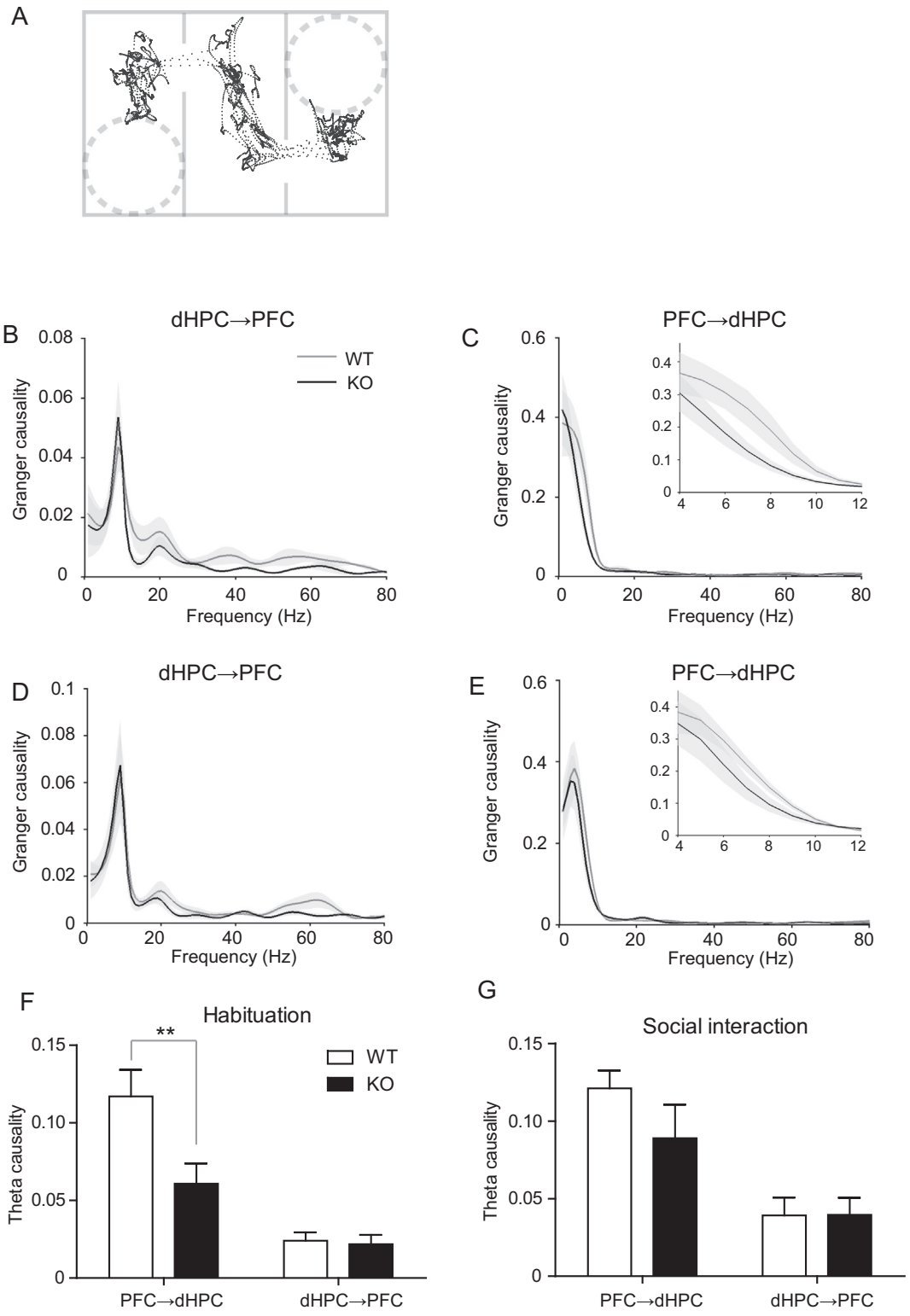

Fig. 7. Causality between dHPC and PFC during social interaction (KO: $N = 10$; WT: $N = 7$). (A) Representative video tracking data in a three-chambered social interaction test during 5 min habituation. (B) and (C) Average Granger causality between dHPC and PFC for both directions of dHPC → PFC (B) and PFC → dHPC (C) in *Cx3cr1* knockout mice and their wild-type littermates during habituation. Inset, zoom up at theta range. Average theta PFC → dHPC causality (4–12 Hz) was higher than dHPC → PFC causality. (D) and (E) Average Granger causality during social interaction. (F) and (G) Theta band causality during both habituation (F) and social interaction (G) phase. Wild-type mice showed higher PFC → dHPC theta causality (Bonferroni correction). $^{**}P < 0.01$.

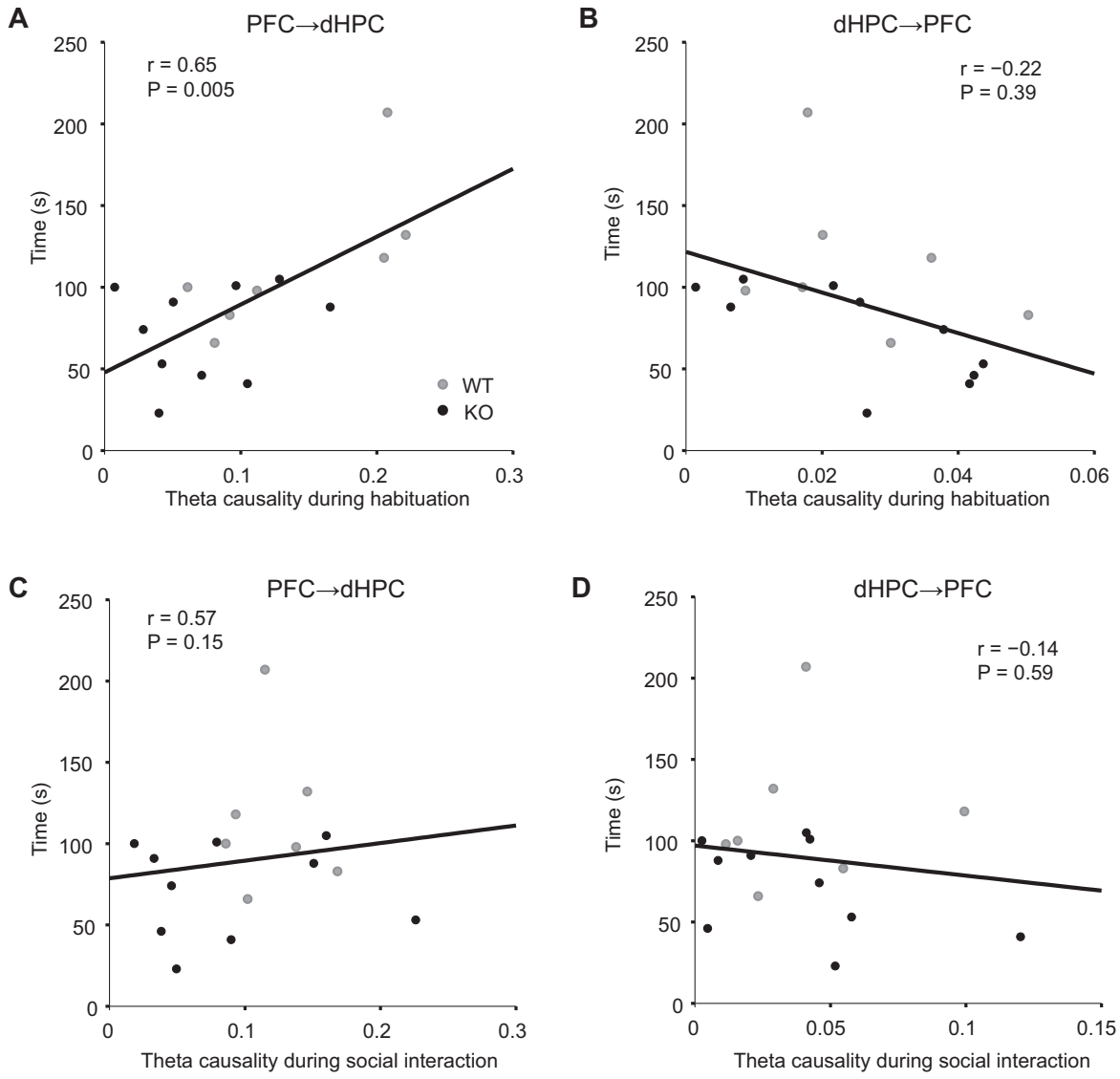

Fig. 8. Pearson correlation between the duration of social interaction and theta causality (KO: $N = 10$; WT: $N = 7$). (A) and (B) Correlation between the time spent investigating a juvenile male mouse and the PFC → dHPC (A) or dHPC → PFC (B) causality during habituation in both wild-type and *Cx3cr1* knockout mice. PFC → dHPC causality was significantly correlated with the interaction time. (C) and (D) Correlation between the social interaction time and the PFC → dHPC (C) or dHPC → PFC (D) causality during social interaction. The theta causality during the social interaction phase was not correlated with the interaction time.

directional deficits in PFC–dHPC connectivity occurred in PFC → dHPC direction but not in dHPC → PFC direction. This demonstrates that PFC to dHPC driving is impaired in *Cx3cr1* knockout mice and failed transmission of information processing from the PFC is probably a baseline problem in the prefrontal–hippocampal direction. Furthermore a positive correlation between the social interaction behavior and the PFC → dHPC causality was found. Together with other studies of manipulating PFC neurons to modulate social behavior (Avale et al., 2011; Yizhar et al., 2011), the current data suggest that neural activities driven from the PFC could underlie the prefrontal executive and cognitive functions for exploring and responding to social stimuli (Dalley et al., 2004).

Synchronization between the PFC and the dHPC has been widely reported in free exploration (Siapas et al., 2005; Colgin, 2011) and increased theta PFC–dHPC coherence occurred upon learning the spatial working memory task (Benchenane et al., 2010). Anatomically there are no direct projections between the PFC and the dHPC and disrupted PFC driving to the dHPC may occur through middle thalamic areas, such as mediodorsal thalamus (Parnaudeau et al., 2013) or nucleus reuniens (Xu and Südhof, 2013).

The Granger causality is a powerful tool in analyzing directed oscillatory activities in different brain structures. Estimation of the causality is built on multivariate linear regression model and the application of causality analysis requires careful and appropriate choice of the model order. The use of AR model could adequately capture the spectral measurement of LFPs and it has been previously applied in LFP causal analysis

(Brockmann Marco et al., 2011; Herrojo Ruiz et al., 2014; Zavala et al., 2014). Using two anxiety tests and social interaction test, pronounced driving relationship between the HPC and the PFC was found, highlighting the task-dependent roles of directed vHPC–PFC oscillations during anxiety and directed dHPC–PFC oscillations during social interaction respectively. Future work could combine the optogenetic or pharmacogenetic tools with *in vivo* electrophysiology to dissect the specific neuronal projections and test whether manipulating the neuronal transmissions could be accompanied by the information flow changes revealed by the Granger causality. Such circuit manipulation can contribute to the understanding of how the directed oscillatory activities are generated by the circuit and how they are linked to the modulation of behavior.

Acknowledgments—The author would like to thank EMBL mouse facility for expert mouse husbandry, the EMBL Phenotyping Facility for assistance in experiments. This work was supported by EMBL Interdisciplinary Postdoc Fellowship (EIPOD) and Basic Research Grant of Shenzhen city government (JCYJ20140901003938992) and Shenzhen Engineering Laboratory for Brain Activity Mapping Technologies.

REFERENCES

Adhikari A, Topiwala MA, Gordon JA (2010) Synchronized activity between the ventral hippocampus and the medial prefrontal cortex during anxiety. Neuron 65:257–269.

Adhikari A, Topiwala Mihir A, Gordon Joshua A (2011) Single units in the medial prefrontal cortex with anxiety-related firing patterns are preferentially influenced by ventral hippocampal activity. Neuron 71:898–910.

Akaike H (1974) A new look at the statistical model identification. IEEE Trans Autom Control 19:716–723.

Amodio DM, Frith CD (2006) Meeting of minds: the medial frontal cortex and social cognition. Nat Rev Neurosci 7:268–277.

Anthony Todd E, Dee N, Bernard A, Lerchner W, Heintz N, Anderson David J (2014) Control of stress-induced persistent anxiety by an extra-amygdala septohypothalamic circuit. Cell 156:522–536.

Avale ME, Chabout J, Pons S, Serreau P, De Chaumont F, Olivo-Marin J-C, Bourgeois J-P, Maskos U, Changeux J-P, Granon S (2011) Prefrontal nicotinic receptors control novel social interaction between mice. FASEB J 25:2145–2155.

Benchenane K, Peyrache A, Khamassi M, Tierney PL, Gioanni Y, Battaglia FP, Wiener SI (2010) Coherent theta oscillations and reorganization of spike timing in the hippocampal–prefrontal network upon learning. Neuron 66:921–936.

Bienvenu Thomas CM, Busti D, Magill Peter J, Ferraguti F, Capogna M (2012) Cell-type-specific recruitment of amygdala interneurons to hippocampal theta rhythm and noxious stimuli in vivo. Neuron 74:1059–1074.

Bird CM, Burgess N (2008) The hippocampus and memory: insights from spatial processing. Nat Rev Neurosci 9:182–194.

Bourin M, Hascoët M (2003) The mouse light/dark box test. Eur J Pharmacol 463:55–65.

Brankačk J, Kukushka VI, Vyssotski AL, Draguhn A (2010) EEG gamma frequency and sleep–wake scoring in mice: comparing two types of supervised classifiers. Brain Res 1322:59–71.

Brockmann Marco D, Pöschel B, Cichon N, Hanganu-Opatz Ileana L (2011) Coupled oscillations mediate directed interactions between prefrontal cortex and hippocampus of the neonatal rat. Neuron 71:332–347.

Brovelli A, Ding M, Ledberg A, Chen Y, Nakamura R, Bressler SL (2004) Beta oscillations in a large-scale sensorimotor cortical network: directional influences revealed by Granger causality. Proc Natl Acad Sci USA 101:9849–9854.

Buzsáki G (2002) Theta oscillations in the hippocampus. Neuron 33:325–340.

Colgin LL (2011) Oscillations and hippocampal–prefrontal synchrony. Curr Opin Neurobiol 21:467–474.

Courchesne E, Redcay E, Morgan JT, Kennedy DP (2005) Autism at the beginning: microstructural and growth abnormalities underlying the cognitive and behavioral phenotype of autism. Dev Psychopathol 17:577–597.

Dalley JW, Cardinal RN, Robbins TW (2004) Prefrontal executive and cognitive functions in rodents: neural and neurochemical substrates. Neurosci Biobehav Rev 28:771–784.

Ding M, Bressler SL, Yang W, Liang H (2000) Short-window spectral analysis of cortical event-related potentials by adaptive multivariate autoregressive modeling: data preprocessing, model validation, and variability assessment. Biol Cybern 83:35–45.

Ding M, Chen Y, Bressler SL (2006) Granger causality: basic theory and application to neuroscience. In: Handbook of Time Series Analysis, pp 437–460. Wiley-VCH Verlag GmbH & Co. KGaA.

Engin E, Treit D (2007) The role of hippocampus in anxiety: intracerebral infusion studies. Behav Pharmacol 18(365–374):3. http://dx.doi.org/10.1097/FBP.1090b1013e3282de7929.

Etholm L, Arabadzisz D, Lipp H-P, Heggelund P (2010) Seizure logging: a new approach to synchronized cable-free EEG and video recordings of seizure activity in mice. J Neurosci Methods 192:254–260.

Friston KJ (1999) Schizophrenia and the disconnection hypothesis. Acta Psychiatr Scand Suppl 395:68–79.

Hen I, Sakov A, Kafkafi N, Golani I, Benjamini Y (2004) The dynamics of spatial behavior: how can robust smoothing techniques help? J Neurosci Methods 133:161–172.

Herrojo Ruiz M, Huebl J, Schönecker T, Kupsch A, Yarrow K, Krauss JK, Schneider G-H, Kühn AA (2014) Involvement of human internal globus pallidus in the early modulation of cortical error-related activity. Cereb Cortex 24:1502–1517.

Hoover W, Vertes R (2007) Anatomical analysis of afferent projections to the medial prefrontal cortex in the rat. Brain Struct Funct 212:149–179.

Jones MW, Wilson MA (2005) Theta rhythms coordinate hippocampal–prefrontal interactions in a spatial memory task. PLoS Biol 3:e402.

Just MA, Keller TA, Malave VL, Kana RK, Varma S (2012) Autism as a neural systems disorder: a theory of frontal-posterior underconnectivity. Neurosci Biobehav Rev 36:1292–1313.

Kheirbek Mazen A, Drew Liam J, Burghardt Nesha S, Costantini Daniel O, Tannenholz L, Ahmari Susanne E, Zeng H, Fenton André A, Hen R (2013) Differential control of learning and anxiety along the dorsoventral axis of the dentate gyrus. Neuron 77:955–968.

Kishi T, Tsumori T, Yokota S, Yasui Y (2006) Topographical projection from the hippocampal formation to the amygdala: a combined anterograde and retrograde tracing study in the rat. J Comp Neurol 496:349–368.

Kjelstrup KG, Tuvnes FA, Steffenach HA, Murison R, Moser EI, Moser MB (2002) Reduced fear expression after lesions of the ventral hippocampus. Proc Natl Acad Sci USA 99:10825–10830.

Lipkind D, Sakov A, Kafkafi N, Elmer GI, Benjamini Y, Golani I (2004) New replicable anxiety-related measures of wall vs. center behavior of mice in the open field. J Appl Physiol 97(1):347–359.

McHugh SB, Deacon RMJ, Rawlins JNP, Bannerman DM (2004) Amygdala and ventral hippocampus contribute differentially to mechanisms of fear and anxiety. Behav Neurosci 118:63–78.

Miller EK, Cohen JD (2001) An integrative theory of prefrontal cortex function. Annu Rev Neurosci 24:167–202.

Parnaudeau S, O'Neill P-K, Bolkan Scott S, Ward Ryan D, Abbas Atheir I, Roth Bryan L, Balsam PD, Gordon Joshua A, Kellendonk C (2013) Inhibition of mediodorsal thalamus disrupts thalamofrontal connectivity and cognition. Neuron 77:1151–1162.

Pettersson-Yeo W, Allen P, Benetti S, McGuire P, Mechelli A (2011) Dysconnectivity in schizophrenia: where are we now? Neurosci Biobehav Rev 35:1110–1124.

Proakis JG, Manolakis DG (1996) Digital signal processing (3rd ed.): principles, algorithms, and applications. Prentice-Hall Inc.
Schipul SE, Keller TA, Just MA (2011) Inter-regional brain communication and its disturbance in autism. Front Syst Neurosci 5.
Seth AK (2010) A MATLAB toolbox for Granger causal connectivity analysis. J Neurosci Methods 186:262–273.
Shah AA, Treit D (2003) Excitotoxic lesions of the medial prefrontal cortex attenuate fear responses in the elevated-plus maze, social interaction and shock probe burying tests. Brain Res 969:183–194.
Shah AA, Sjovold T, Treit D (2004) Inactivation of the medial prefrontal cortex with the GABAA receptor agonist muscimol increases open-arm activity in the elevated plus-maze and attenuates shock-probe burying in rats. Brain Res 1028:112–115.
Siapas AG, Lubenov EV, Wilson MA (2005) Prefrontal phase locking to hippocampal theta oscillations. Neuron 46:141–151.
Sigurdsson T, Stark KL, Karayiorgou M, Gogos JA, Gordon JA (2010) Impaired hippocampal–prefrontal synchrony in a genetic mouse model of schizophrenia. Nature 464:763–767.
Trent NL, Menard JL (2010) The ventral hippocampus and the lateral septum work in tandem to regulate rats' open-arm exploration in the elevated plus-maze. Physiol Behav 101:141–152.
Uhlhaas PJ, Singer W (2010) Abnormal neural oscillations and synchrony in schizophrenia. Nat Rev Neurosci 11:100–113.
Vyssotski AL, Dell'Omo G, Dell'Ariccia G, Abramchuk AN, Serkov AN, Latanov AV, Loizzo A, Wolfer DP, Lipp H-P (2009) EEG responses to visual landmarks in flying pigeons. Curr Biol 19:1159–1166.
Xu W, Südhof TC (2013) A neural circuit for memory specificity and generalization. Science 339:1290–1295.
Yizhar O, Fenno LE, Prigge M, Schneider F, Davidson TJ, O'Shea DJ, Sohal VS, Goshen I, Finkelstein J, Paz JT, Stehfest K, Fudim R, Ramakrishnan C, Huguenard JR, Hegemann P, Deisseroth K (2011) Neocortical excitation/inhibition balance in information processing and social dysfunction. Nature 477:171–178.
Zavala BA, Tan H, Little S, Ashkan K, Hariz M, Foltynie T, Zrinzo L, Zaghloul KA, Brown P (2014) Midline frontal cortex low-frequency activity drives subthalamic nucleus oscillations during conflict. J Neurosci 34:7322–7333.
Zhan Y, Paolicelli RC, Sforazzini F, Weinhard L, Bolasco G, Pagani F, Vyssotski AL, Bifone A, Gozzi A, Ragozzino D, Gross CT (2014) Deficient neuron–microglia signaling results in impaired functional brain connectivity and social behavior. Nat Neurosci 17:400–406.

(Accepted 26 May 2015)
(Available online 30 May 2015)